Inactivation of mitochondrial aspartate aminotransferase contributes to the respiratory deficit of yeast frataxin-deficient cells

Dominika Sliwa, Julien Dairou, Jean-Michel Camadro, Renata Santos

BJ www.biochemj.org

BJ Disease

Biochem. J. (2012) **441**, 945–953 (Printed in Great Britain) doi:10.1042/BJ20111574

Inactivation of mitochondrial aspartate aminotransferase contributes to the respiratory deficit of yeast frataxin-deficient cells

Dominika SLIWA*, Julien DAIROU†, Jean-Michel CAMADRO* and Renata SANTOS*[1]

*Institut Jacques Monod, CNRS-Université Paris Diderot, Sorbonne Paris Cité, 15 rue Hélène Brion, 75205 Paris cedex 13, France, and †Unité BFA (EAC 4413), Université Paris Diderot, Sorbonne Paris Cité-CNRS, 4 rue Marie Andrée Lagroua Weill Halle, 75205 Paris Cedex 13, France

Friedreich's ataxia is a hereditary neurodegenerative disease caused by reduced expression of mitochondrial frataxin. Frataxin deficiency causes impairment in respiratory capacity, disruption of iron homoeostasis and hypersensitivity to oxidants. Although the redox properties of NAD (NAD^+ and NADH) are essential for energy metabolism, only few results are available concerning homoeostasis of these nucleotides in frataxin-deficient cells. In the present study, we show that the malate–aspartate NADH shuttle is impaired in *Saccharomyces cerevisiae* frataxin-deficient cells ($\Delta yfh1$) due to decreased activity of cytosolic and mitochondrial isoforms of malate dehydrogenase and to complete inactivation of the mitochondrial aspartate aminotransferase (Aat1). A considerable decrease in the amount of mitochondrial acetylated proteins was observed in the $\Delta yfh1$ mutant compared with wild-type. Aat1 is acetylated in wild-type mitochondria and deacetylated in $\Delta yfh1$ mitochondria suggesting that inactivation could be due to this post-translational modification. Mutants deficient in iron–sulfur cluster assembly or lacking mitochondrial DNA also showed decreased activity of Aat1, suggesting that Aat1 inactivation was a secondary phenotype in $\Delta yfh1$ cells. Interestingly, deletion of the *AAT1* gene in a wild-type strain caused respiratory deficiency and disruption of iron homoeostasis without any sensitivity to oxidative stress. Our results show that secondary inactivation of Aat1 contributes to the amplification of the respiratory defect observed in $\Delta yfh1$ cells. Further implication of mitochondrial protein deacetylation in the physiology of frataxin-deficient cells is anticipated.

Key words: frataxin, Friedreich's ataxia, malate–aspartate NADH shuttle, mitochondrion, protein acetylation, yeast.

INTRODUCTION

FA (Friedreich's ataxia) is the most common autosomal recessive inherited ataxia. It is a slowly progressive neurodegenerative disease that affects the central and peripheral nervous system. Other organs can be affected in FA; 60 % of patients develop cardiomyopathy and almost 40 % of patients present diabetes or glucose intolerance [1]. The most common mutation observed in FA patients is an unstable hyperexpansion of a GAA trinucleotide repeat in the first intron of the *FXN* gene that leads to the formation of a non-usual B-DNA structure and heterochromatin conformation that causes transcriptional silencing [2,3]. The consequence is decreased expression of the encoded protein, frataxin [4]. Frataxin is a small mitochondrial matrix protein that participates in iron–sulfur cluster assembly [5]. Frataxin deficiency induces a decrease in the activities of iron–sulfur cluster enzymes and in respiratory capacity, perturbation of cellular iron homoeostasis and hypersensitivity to oxidants [6]. Therefore major phenotypes of frataxin deficiency are related to energy metabolism and antioxidant response. Although pyridine nucleotides NAD (NAD^+ and NADH) and NADP ($NADP^+$ and NADPH) are electron carriers essential for energy production and defence against oxidative stress, little is known about the regulation of their pools in frataxin-deficient cells. We showed previously that the NADPH/$NADP^+$ ratio was considerably lower in the yeast *Saccharomyces cerevisiae* frataxin-deficient mutant ($\Delta yfh1$) compared with wild-type, which, in addition to the disturbed glutathione redox status, contributed to the severe oxidative stress condition observed in $\Delta yfh1$ cells [7]. Another study showed that the levels of reduced glutathione, ATP, NADPH and NADH were significantly increased in the heart of transgenic mice ubiquitously overexpressing frataxin compared with control animals, indicating enhanced mitochondrial energy conversion and antioxidant defence capacity with increasing frataxin levels [8].

Besides being an enzymatic oxidoreductase cofactor, NAD^+ is the substrate of enzymes that catalyse protein modification reactions. In particular, the SIRT (sirtuin)-mediated protein deacetylation and the ADP-ribosylation, catalysed by PARP [poly(ADP-ribose) polymerase] family, regulate gene expression, DNA repair, aging, calcium signalling, generation of ROS (reactive oxygen species) and cell death [9,10]. In yeast, NAD^+ biosynthesis involves a *de novo* pathway from tryptophan and several salvage pathways from various precursors, such as nicotinic acid mononucleotide and nicotinamide riboside [11]. NAD^+ biosynthesis appears to occur outside the mitochondria because all enzymes are localized in the cytosol and the nucleus, with the exception of Bna4, which is a mitochondrial kynurenine 3-mono-oxygenase required for *de novo* NAD^+ synthesis from kynurenine. This implies that NAD^+ must be imported into the mitochondria. Two mitochondrial NAD^+ transporters, Ndt1 and Ndt2, perform this function [12]. In addition, reducing equivalents from NADH can be exchanged between the cytosol and the mitochondria by NADH shuttles, such as the glycerol 3-phosphate shuttle, the ethanol–acetaldehyde shuttle and the malate–aspartate shuttle [13,14]. The glycerol 3-phosphate shuttle only oxidizes cytosolic NADH transferring the electrons directly to the respiratory chain. This shuttle has two components, the cytosolic glycerol-3-phosphate dehydrogenase (Gpd1/2) and the inner mitochondrial membrane glycerol-3-phosphate dehydrogenase (Gut2). The ethanol–acetaldehyde shuttle is composed of

Abbreviations used: 2D, two-dimensional; DTT, dithiothreitol; FA, Friedreich's ataxia; G3PDH, glyceraldehyde-3-phosphate dehydrogenase; HA, haemagglutinin; LDH, lactate dehydrogenase; PHO, phosphate-responsive signalling; PL, pyridoxal; PLP, pyridoxal 5′-phosphate; PM, pyridoxamine; PN, pyridoxine; ROS, reactive oxygen species; SIRT, sirtuin; TCA, tricarboxylic acid.

[1] To whom correspondence should be addressed (email santos.renata@ijm.univ-paris-diderot.fr).

mitochondrial alcohol dehydrogenase (Adh3) that converts ethanol into acetaldehyde, producing NADH and the cytosolic isoforms (Adh1/2) that perform the inverse reaction and synthesize NAD^+ in the cytosol. Acetaldehyde and ethanol freely diffuse through mitochondrial membranes. The yeast malate–aspartate shuttle components include mitochondrial and cytosolic malate dehydrogenase (Mdh1/2) and aspartate aminotransferase (Aat1/2) and the mitochondrial aspartate/glutamate exchanger Agc1 [15]. In yeast, sugar metabolism and biomass production (synthesis of amino acids, nucleic acids and reduced lipids) result in NADH generation in the cytosol [13,14]. For the most part of cytosolic NADH, reoxidation to NAD^+ takes place in the mitochondria by the electron transport chain [14]. Under conditions where respiration is repressed, glycerol production provides NAD^+ regeneration in the cytosol [14]. Therefore NADH shuttles are required for maintaining the NAD^+/NADH ratios in the mitochondrial and cytosolic NAD pools. The biological importance of this function is evident from the calorie restriction-induced lifespan extension in yeast [16] and by the brain hypomyelination and cortex neuron abnormalities in Aralar1 (mitochondrial aspartate/glutamate transporter)-knockout mice [17]. In the present study, we concentrated on NAD metabolism in the yeast Δ*yfh1* mutant.

MATERIALS AND METHODS

Yeast strains and growth conditions

The *S. cerevisiae* strains used in the present study were derived from YPH499 cycloheximide-resistant (wild-type; MATa *ura3-52 lys2-801 ade2-101 trp1-Δ63 his3-Δ200 leu2-Δ1 cyh2*); YPH499Δ*yfh1* (Δ*yfh1*::*TRP1*), YPH499Δ*aat1* (Δ*aat1*::*HIS3MX6*), YPH499*AAT1-HA* and YPH499*nfs1-14* [18]. To prevent the accumulation of suppressor mutations, the Δ*yfh1* mutant was constructed using the YPH499 *yfh1* shuffle strain [19]. In the shuffle strain, the *yfh1* deletion is covered by pRS318-*YFH1*, a plasmid containing the CEN, *CYH2* and the *YFH1* HindIII genomic fragment. The plasmid was removed before experiments by counterselection on YPRaf medium (1 % yeast extract, 2 % Bacto peptone, 2 % raffinose and 0.1 % glucose) containing 10 μg/ml cycloheximide, which is toxic in the presence of the *CYH2* allele. For the construction of the Δ*aat1*::*HIS3MX6* strain, the *AAT1* coding region was replaced by the *HIS3MX6* gene, which was amplified from plasmid pFA6a-HIS3MX6 by PCR with 5′-TTTGAAAATTACTATCCGTTTTTCACTGCCGAAAGACTTGCGGATCCCCGGGTTAATTAA-3′ and 5′-TAAAAAAATAAAGACAAAGGTGAACTGTAAGGTGAAAAAAGAATTCGAGCTCGTTTAAAC-3′ primers and used for transformation [20]. Successful integration was verified using primers external to the genomic region deleted (5′-GACGATAGCGGATTGAACGA-3′ and 5′-AGTTGGCTAGCGCTAGCTTT-3′). The Aat1 protein was tagged with three tandem copies of the influenza virus HA (haemagglutinin) epitope at the very C-terminus. The HA epitope tags for *AAT1* was amplified from the template pFA6a-3HA-HIS3MX6 as described previously [20], using the following primers: 5′-TGAATCTCTTGAAGCAGTCTCGAAAATGGACAAACTCGCACGGATCCCCGGGTTAATTAA-3′ and 5′-TAAAAAAATAAAGACAAAGGTGAACTGTAAGGTGAAAAAAGAATTCGAGCTCGTTTAAAC-3′. Successful integration was verified using the external primers 5′-CGGAGTCAATGATTCGAACG-3′ and 5′-AGTTGGCTAGCGCTAGCTTT-3′. To generate a strain carrying deletions in the mitochondrial DNA (herein called ρ^0 strain), cells were grown for 24 h in defined medium (yeast nitrogen base supplemented with the required amino acids, 2 % glucose and 200 μg/ml adenine) containing 10 μg/ml ethidium bromide, 1/100 diluted in the same medium and treated for another 24 h. Isolated clones were verified by genetic crossing with ρ^0 tester strains and plating on YPGly medium (1 % yeast extract, 2 % Bacto peptone and 2 % glycerol). Unless stated all experiments were carried out in YPD medium (1 % yeast extract, 2 % Bacto peptone and 2 % D-glucose) at 30 °C. All media were supplemented with 200 μg/ml adenine. For growth under anaerobic conditions, the medium was supplemented with 30 mg/l ergosterol and 2 ml/l Tween 80 (Jacomex anaerobic glove box; oxygen concentration below 5 p.p.m.).

Cell fractionation

Mitochondrial and extra-mitochondrial fractions were prepared from stationary-phase cultured cells (D_{600} ~4) in YPD medium. Cell pellets were resuspended in ice-cold 50 mM potassium phosphate buffer, pH 7.4, and 0.6 M sorbitol in the presence of protease inhibitors (Roche), disrupted using glass beads (0.45–0.55 mm diameter, Sartorius StedimBiotech) and centrifuged at 4 °C for 5 min at 1000 ***g***, to remove glass beads, unbroken cells and cell wall debris. The resulting supernatant was centrifuged at 4 °C for 20 min at 10000 ***g***. The supernatant corresponds to the extra-mitochondrial fraction containing cytosolic, nuclear and vacuolar proteins. The pellet containing the mitochondria was rinsed twice and resuspended in the same buffer. The protein content was determined using the Bradford assay and BSA as the standard. The samples were frozen in a solid CO_2/ethanol bath and stored at − 80 °C. The quality of the mitochondrial and extra-mitochondrial fractions was monitored by Western blotting using the anti-porin antibody (mitochondrial protein) and anti-(phosphoglycerate kinase) antibody (cytosolic protein); samples that had less than 10 % contamination were kept. However, contamination with vacuolar proteins [monitored using anti-(carboxypeptidase Y) antibody] can be as high as 20 % in some mitochondrial samples.

Enzymatic activities

Enzymatic activities were assayed spectrophotometrically at 340 nm using crude mitochondrial and extra-mitochondrial fractions. To ensure an efficient disruption of mitochondrial membranes, assays were carried out in the presence of 0.1 % Triton X-100. Aspartate aminotransferase activity was measured indirectly as the rate of the oxidation of NADH by malate dehydrogenase. The reagent mixture contained 130 mM aspartate, 6.6 mM 2-oxoglutarate, 0.24 mM NADH, 5 units/ml malate dehydrogenase, 1.5 unit/ml LDH (lactate dehydrogenase) and 50 mM potassium phosphate buffer, pH 7.4. Malate dehydrogenase was assayed in 50 mM potassium phosphate buffer, pH 7.4, 0.6 mM oxaloacetate and 0.24 mM NADH. Activities of alcohol dehydrogenase and G3PDH (glyceraldehyde-3-phosphate dehydrogenase) were monitored by the rate of NAD^+ reduction. Alcohol dehydrogenase activity was assayed in 0.1 M sodium pyrophosphate buffer, pH 9.2, 0.2 M ethanol and 0.25 mM NAD^+, and G3PDH activity was assayed in 0.015 M sodium pyrophosphate buffer containing 0.03 M sodium arsenate, pH 8.5, in the presence of 0.25 mM NAD, 3 mM DTT (dithiothreitol) and 0.5 mM D, L-glyceraldehyde 3-phosphate. Aconitase and succinate dehydrogenase activities were assayed as described previously [21,22].

Immunoprecipitation and Western blotting

For immunoprecipitation, isolated mitochondria were lysed in 50 mM Hepes, pH 7.4, 150 mM NaCl, 0.5 % NP-40 (Nonidet

P40) and 10 % glycerol in the presence of protease inhibitors (Roche), incubated for 5 h at 4 °C with anti-acetylated lysine antibody (Cell Signaling Technology) or anti-HA antibody (Santa Cruz Biotechnology) and another 1 h of incubation with magnetic beads coupled with Protein G (Adamtech). The beads were washed three times with the lysis buffer and resuspended in Laemmli sample buffer without 2-mercaptoethanol, boiled for 5 min and subjected to Western blotting. For Western blot analysis, denaturated protein samples in Laemmli buffer were separated by SDS/PAGE (10 % gel) and the protein bands were electrotransferred on to a Hybond nitrocellulose membrane (GE Healthcare). Primary anti-HA (Santa Cruz Laboratory), anti-(phosphoglycerate kinase) (Molecular Probes), anti-porin (Invitrogen) and anti-(acetylated lysine) (Cell Signaling Technology, reference 9681 for Western blotting) monoclonal antibodies and anti-(acetylated lysine) (Cell Signaling Technology, reference 9681 for immunoprecipitation) polyclonal antibody were detected after incubation with peroxidase-conjugated secondary antibody, with chemiluminescent substrate (Supersignal West from Pierce).

2D (two-dimensional) gel electrophoresis

The first dimension of 2D gel electrophoresis was performed on a precast Immobiline DryStrip pH 3–11 NL, 7 cm (non-linear immobilized pH 3–11 gradient gel; GE Healthcare) using Multifor II System according to the manufacturer's instructions. The gels were loaded with 70 μg of mitochondrial protein samples. Isoelectric focusing was followed by separation in a 10 % polyacrylamide gel and Western blot analysis.

Metabolite analysis

The intracellular levels of NAD^+ and NADH were measured fluorimetrically (λ_{ex} at 340 nm, λ_{em} at 460 nm) using yeast alcohol dehydrogenase and LDH reactions respectively. To prepare the whole-cell extracts, cells were harvested at the exponential phase of growth (D_{600} ~0.8), resuspended in 50 mM Tris/HCl buffer, pH 7.4, and disrupted using glass beads. For NAD^+ analysis, samples were submitted to acidic extraction by addition of perchloric acid to a final concentration of 0.2 M. The precipitated proteins were removed by centrifugation and the resulting supernatant was neutralized with KOH. NAD^+ pools were measured in 0.1 M pyrophosphate buffer, pH 9.2, in the presence of 0.5 % ethanol; 1 unit/ml alcohol dehydrogenase was added and the increase in fluorescence intensity was recorded until it reached a plateau. For NADH measurements, the same samples were alkalized with KOH (0.05 M final concentration) and incubated for 10 min at 60 °C. Samples (10–50 μl) were added to 2 ml of reagent mixture (0.1 M triethanolamine/HCl, pH 7.4, and 1.5 mM pyruvate). The conversion of NADH into NAD^+ was catalysed by 1 unit/ml LDH. CoA and acetyl-CoA were analysed by reversed-phase HPLC (Shimadzu HPLC system interfaced with the LabSolution software). Samples were injected on to a Kromasil Eternity C_{18} column (length, 250 nm; internal diameter, 4 mm; particle size, 5 μm) at 40 °C. The mobile phase used for the separation consisted of two eluants: solvent A was 20 mM sodium perchlorate buffer (pH 3.0), and solvent B was acetonitrile. Compounds were separated by the following discontinuous gradient at a flow rate of 1.5 ml/min: the initial concentration of 5 % in solvent B increased to 20 % over 2.5 min and remained stable for 2.5 min; this was followed by a decrease to 5 % over the next 1 min, and the initial conditions were then maintained for 5 min. The products were monitored spectrophotometrically at 254 and 280 nm and quantified by integration of the peak absorbance area, employing a calibration curve established with various known concentrations of CoA and acetyl-CoA. B_6 vitamers were also determined by HPLC with fluorescence detection as previously described [23].

Other techniques

Iron uptake was measured in microtitre plates. Overnight cultures were diluted to a D_{600} of 0.2 in 10 ml of YPD medium, grown for 4.5 h until the D_{600} reached 1.0, centrifuged and resuspended in 2 ml of 50 mM citrate and 5 % glucose. A 200 μl aliquot was dispensed in microtitre plates in quadruplicate, 1 μM [^{55}Fe]ferrichrome was then added and the plate was incubated for 30 min at 30 °C. The cells were collected with a cell harvester (Brandel) and washed on the filter before scintillation counting. Cytochrome content and respiration were measured in cells grown in YPRaf medium. Low-temperature absorption spectra (− 191 °C) of whole cells were recorded as described previously [19]. The respiratory activity of isolated mitochondria was measured with a 1 ml thermostatically controlled oxypolarographic cell equipped with a Clark-type electrode. Oxygen consumption was measured in 10 mM Tris/HCl, pH 6.8 (containing 0.65 M sorbitol, 0.36 mM EDTA, 10 mM KCl and 10 mM KH_2PO_4), saturated with air at 30 °C (234 nmol/ml dissolved O_2). The electron donors for respiration were 1 mM NADH and 10 mM succinate.

RNA isolation and real-time quantitative PCR analysis

Total RNA for real-time quantitative PCR analysis was extracted from stationary-phase cultured cells using the hot phenol method as described previously [7] and purified using Qiagen columns (RNeasy kit). Real-time quantitative PCR analysis was performed as previously described using *ACT1* mRNA for normalization [24]. The *AAT1* primer sequences were 5′-TCCACCAGGATACGGTTCTC-3′ and 5′-CCACCCTAGACGGTCAAACA-3′. The relative expression in Δ*yfh1*/wt cells was calculated using the equation described by Pfaffl [25]. The results reported were obtained from three biological replicates and PCR runs were repeated twice.

Statistical analysis

All values are means ± S.D. for biological triplicates. All experiments were repeated at least twice. Statistical analysis was performed using a paired Student's *t* test.

RESULTS

Mitochondrial aspartate aminotransferase activity is severely reduced in Δ*yfh1* cells

Under aerobic and high-glucose conditions, *S. cerevisiae* cells have a mixed metabolism relying on fermentation and respiration. Several redox shuttles translocate electrons across the inner mitochondrial membrane resulting in oxidation of NADH in the cytosol and reduction of NAD^+ in the mitochondria. To determine how the low respiratory activity of Δ*yfh1* cells affects the components of NADH shuttles, the activities of G3PDH, alcohol dehydrogenase, malate dehydrogenase and aspartate aminotransferase were measured in mitochondrial and extra-mitochondrial (herein named cytosolic) fractions. No significant difference was observed in the activities of cytosolic and mitochondrial G3PDH in wild-type and Δ*yfh1* mutant cells (Figure 1). A statistically significant ($P < 0.001$) increase in both mitochondrial and cytosolic alcohol dehydrogenase activities was detected in the Δ*yfh1* mutant compared with wild-type cells (Figure 1). These results suggest that ethanol fermentation is

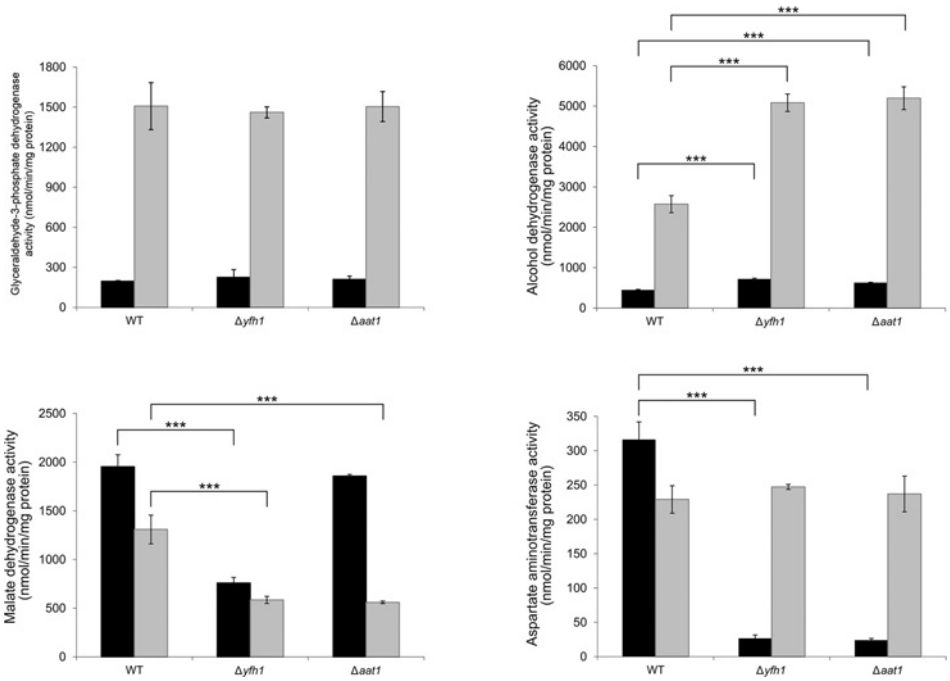

Figure 1 Activity of NADH shuttle enzymes in Δ*yfh1*, Δ*aat1* and wild-type mitochondria and cytosol

Activities of G3PDH, alcohol dehydrogenase, malate dehydrogenase and aspartate aminotransferase in mitochondrial and cytosolic fractions. Black bars, mitochondria; grey bars, cytosol. Results are means ± S.D. ($n = 3$ or 4; $^{***}P < 0.001$).

induced in Δ*yfh1* cells, but not glycerol production. Malate dehydrogenase activity was previously shown to be slightly affected in Δ*yfh1* mutants [26]. Under the conditions used in the present study, the malate dehydrogenase activities of mitochondrial and cytosolic isoforms were decreased more than 2-fold in the Δ*yfh1* mutant compared with wild-type (Figure 1). Although the cytosolic aspartate aminotransferase activity was normal in Δ*yfh1* cells, the activity of the mitochondrial isoform was less than 10 % of the value determined for wild-type cells. Indeed, a comparable residual activity was also detected in the mutant deficient for the mitochondrial aspartate aminotransferase (Δ*aat1*) and corresponds to the contaminating cytosolic isoform (Figure 1). These results show that the malate–aspartate shuttle is severely affected in the Δ*yfh1* mutant due to the deficit in mitochondrial aspartate aminotransferase activity and decreased malate dehydrogenase activities.

As observed for Δ*yfh1*, Δ*aat1* cells also showed increased mitochondrial and cytosolic alcohol dehydrogenase activities but no difference in G3PDH activity (Figure 1). This could be explained by increased ethanol fermentation in Δ*yfh1* and Δ*aat1* cells to compensate for reduced respiration (see below for Δ*aat1* results). The decrease in cytosolic malate dehydrogenase activity in Δ*yfh1* cells could be due to the lack of Aat1 since the same decrease in activity was also observed in Δ*aat1* cells (Figure 1). However, regarding the mitochondrial malate dehydrogenase isoform, a decrease in activity was only observed in Δ*yfh1* cells and could result from a general decline in the oxidative phosphorylation and the tricarboxylic acid cycle or to post-translational modifications (see below).

Influence of deficiency in iron–sulfur clusters, loss of mitochondrial DNA and oxidative stress in mitochondrial aspartate aminotransferase activity

Major phenotypes of yeast Δ*yfh1* include deficiency in iron–sulfur clusters, loss of mitochondrial DNA and sensitivity to oxidants. Therefore we tested whether these conditions could result in decreased Aat1 activity. Indeed, cells deficient in cysteine desulfurase activity (essential for iron–sulfur cluster biosynthesis; *nfs1-14* mutant) and cells lacking complete mitochondrial genome (ρ^0 mutant) showed reduced Aat1 activity, but no significant difference in the activity of the cytosolic isoform (Figure 2A). Treatment of wild-type cells for 6 h with 2 mM H_2O_2, 2 mM paraquat or 0.4 mM menadione did not result in any change in Aat1 activity (results not shown). In addition, under anaerobic conditions, Δ*yfh1* and wild-type cells showed identical activities of cytosolic and mitochondrial aspartate aminotransferase isoforms (Figure 2B). In conclusion, the reduced Aat1 activity could be a secondary effect of iron–sulfur cluster deficiency, loss of mitochondrial DNA and aerobic metabolism in Δ*yfh1* cells.

Loss of mitochondrial aspartate aminotransferase causes disruption of iron metabolism and reduced respiratory activity

To understand what the cellular effects of Aat1 deficiency are, we analysed in detail Δ*aat1* mutant phenotypes. Cellular iron uptake was measured using [^{55}Fe]ferrichrome which is imported by the Arn1 transporter and is a *bona fide* marker of the status of Aft1-regulated genes [27]. A small, but significant, increase (1.8-fold; $P < 0.001$) in cellular iron uptake was detected in Δ*aat1* compared with wild-type cells (Figure 3A). Activities of aconitase and succinate dehydrogenase, which are iron–sulfur cluster-dependent enzymes, were also significantly decreased in Δ*aat1* mitochondria (Figure 3B). Cytochrome content, detected by low-temperature spectra, was also altered in the Δ*aat1* mutant compared with wild-type (Figure 3C). The spectrum was similar to that observed for ρ^0 mutants showing low content of cytochromes *a*, *a3* and *b*. However, no increase in loss of mitochondrial DNA was observed in the Δ*aat1* mutant compared with wild-type (results not shown). In addition, a clear decrease

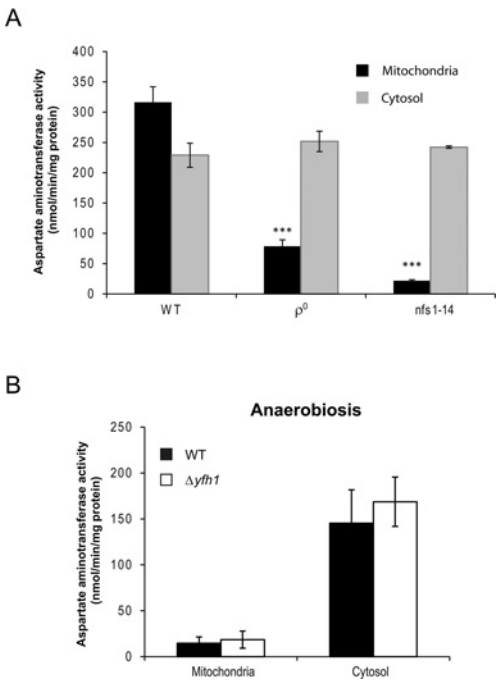

Figure 2 Deficiency in iron–sulfur clusters and loss of mitochondrial DNA cause a decrease in the activity of mitochondrial aspartate aminotransferase

Activities of mitochondrial and cytosolic aspartate aminotransferase in (**A**) ρ^0 and *nfs1* mutants and (**B**) anaerobic Δ*yfh1* and wild-type cells. Results are means ± S.D. ($n = 2$–4; $^{***}P < 0.001$).

in oxygen uptake was observed, using 1 mM NADH and 10 mM succinate as substrates, in Δ*aat1* compared with wild-type cells (Figure 3D). The reduced respiratory capacity was also evident from the poor growth of Δ*aat1* cells in rich media containing glycerol as the sole carbon source (Figure 3E). However, the Δ*aat1* mutant did not show any sensitivity to H_2O_2 (Figure 3E).

These results show that deficiency in Aat1 causes a reduction in respiration and disturbs mitochondrial iron metabolism, as evidenced by decreased activity of iron–sulfur cluster enzymes, loss of cytochromes and increased cellular iron content. As expected, these phenotypes are milder than those observed for Δ*yfh1* cells (Figure 3), but suggest that secondary Aat1 deficiency could exacerbate the respiratory defect in these cells. However, a striking observation in Δ*aat1* cells was the retention of mitochondrial DNA and resistance to oxidative stress, which are generally not conserved in yeast mutants that show affected mitochondrial functions.

NAD^+/NADH pools in Δ*yfh1* and Δ*aat1* cells

The levels of total intracellular NAD^+ and NADH were measured in exponential ($D_{600} \approx 1$) Δ*yfh1* and Δ*aat1* cells, (Table 1). Unexpectedly, in Δ*yfh1* cells, an increase of more than 2-fold was detected in both NAD^+ and NADH levels. This could be a cellular response to the state of constitutive oxidative stress in mutant cells. Two studies reported that treatment of wild-type cells with H_2O_2 induced an increase in total $NAD^+ + NADH$ levels [28,29]. In addition, the salvage pathway appears to be necessary for this increase under oxidative stress conditions [29]. Another possibility is related to phosphate signalling. Recent findings uncovered a link between the PHO (phosphate-responsive signalling) pathway and NAD^+ metabolic pathways mediated by nicotinamide riboside [30]. Wild-type cells grown in low-phosphate medium presented a significant increase in the level of nicotinamide riboside, an NAD^+ precursor. This is in agreement with our previous results showing a deficit in soluble phosphate in Δ*yfh1* cells due to precipitation in the mitochondria and deregulation of the PHO pathway [24]. Another possibility could be that NAD^+/NADH utilization pathways are lowered in mutant cells. One of these pathways is the synthesis of $NADP^+$/NADPH from NAD^+/NADH. Indeed, Δ*yfh1* cells have been shown to have a 2.4-fold reduction in total $NADP^+$/NADPH levels [7]. Altogether, oxidative stress, iron phosphate precipitation and/or reduced NADP levels could contribute to the increased levels of NAD observed in Δ*yfh1* cells. In the case of the Δ*aat1* mutant, no significant difference was observed in NAD^+ and NADH levels compared with wild-type cells (Table 1). This is consistent with the observation that deletion of the Ndt1- and Ndt2-encoding genes did not result in a significant difference in the cellular nucleotide levels in high-glucose media [31]. However, a displacement in the distribution of NAD^+ was observed, with lower cytosolic and higher mitochondrial levels. A reduction in the NAD^+/NADH ratio was detected in both Δ*yfh1* and Δ*aat1* mutants and reflects the poor respiratory activity observed in these strains.

Mitochondrial aspartate aminotransferase is deacetylated in Δ*yfh1*

We addressed the question of why Aat1 activity is inhibited in Δ*yfh1* cells. Transcription of the *AAT1* gene was 4-fold decreased in Δ*yfh1* compared with wild-type cells (Δ*yfh1*/wt ratio, 0.25 ± 0.09). Strains were then constructed containing the Aat1 protein HA-tagged at the C-terminus in the wild-type and Δ*yfh1* context. In these strains, Aat1 activities were not modified compared with non-tagged wild-type and Δ*yfh1* cells indicating that the Aat1–HA enzyme remained functional (Figure 4A). Surprisingly, no considerable reduction in the amount of protein level was detected after Western blotting using an anti-HA antibody (Figure 4B). Moreover, a single distinct band was visible in Western blots excluding several protein modifications that result in a mass change detectable by this technique. We tested whether the oxidation/reduction state of Aat1 protein could be involved by treating the mitochondrial extracts for 10 min with 500 μM DTT before activity measurements; no change in the activities of Aat1 was observed in wild-type and Δ*yfh1* cells (results not shown).

Aspartate aminotransferases are PLP (pyridoxal 5′-phosphate)-containing enzymes; we therefore investigated whether the cofactor was misplaced or lacking in Δ*yfh1* cells. Vitamin B_6 refers to a group of six compounds, PL (pyridoxal), PN (pyridoxine), PM (pyridoxamine) and their respective 5′-phosphorylated derivatives. PLP is the biochemically active cofactor that can readily be synthesized from the other five vitamers by the salvage pathway [32]. *In vitro* incubation of mitochondrial extracts with 0.5 mM PLP before enzymatic activity determination did not lead to an increase in Aat1 activity (results not shown). In addition, no significant difference was observed in PLP levels determined by HPLC between Δ*yfh1* and wild-type cells (Figure 5). However, mitochondrial pools of PL, PN and PM were reduced, although not significantly, in Δ*yfh1* compared with wild-type cells. PM has also an antioxidant function in the cell [33]. Possibly this decrease is the consequence of the constitutive oxidative state condition of Δ*yfh1* cells. Nevertheless cytosolic and mitochondrial PLP pools were not affected in Δ*yfh1* cells, suggesting that inactivation of the enzyme was not due to lack of cofactor.

The Aat1 profile obtained using 2D gel electrophoresis revealed the presence of additional isoforms in the wild-type mitochondria

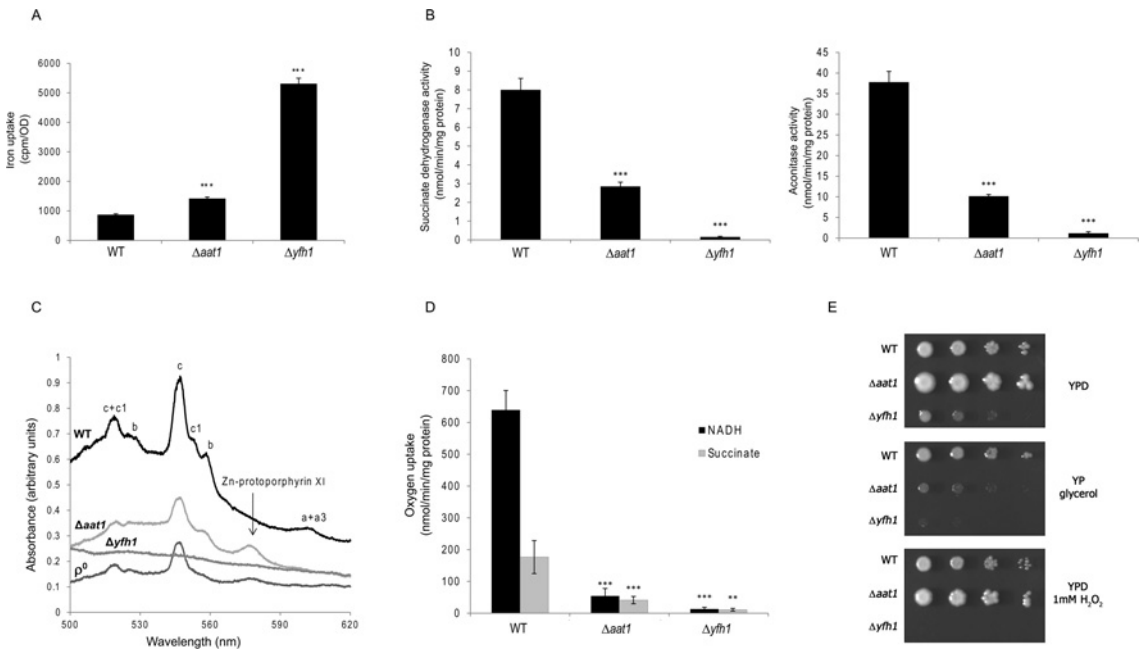

Figure 3 Iron metabolism, respiration and oxidative stress-related phenotypes of Δ*aat1* cells

(**A**) Iron uptake from 1 μM ferrichrome. (**B**) Mitochondrial aconitase and succinate dehydrogenase activities. (**C**) Cytochrome content (low-temperature spectra). (**D**) Mitochondrial oxygen uptake using 1 mM NADH and 10 mM succinate as respiratory substrates. (**E**) Growth on glycerol substrate and sensitivity to 1 mM H_2O_2. Five-fold dilutions of $D_{600} = 3.0$ cell suspensions were spotted on to different media and incubated for 3–4 days at 30 °C. Results are means ± S.D. ($n = 3$; $^{**}P < 0.01$, $^{***}P < 0.001$) or one representative experiment from three performed.

Table 1 Intracellular NAD levels in wild-type, Δ*yfh1* and Δ*aat1* cells

Results are means ± S.D. ($n = 3$; $^{*}P < 0.05$; $^{**}P < 0.01$; $^{***}P < 0.001$).

Strain	NAD^+ (nmol/mg of protein)	NADH (nmol/mg of protein)	NAD^+/NADH ratio
Total			
WT	23.1 ± 2.00	11.2 ± 0.59	2.1 ± 0.06
Δ*yfh1*	48.0 ± 5.75**	33.7 ± 4.35***	1.4 ± 0.03***
Δ*aat1*	20.2 ± 1.00	13.0 ± 1.70	1.6 ± 0.24*
Cytosol			
WT	24.0 ± 0.84	29.9 ± 1.72	0.8 ± 0.01
Δ*yfh1*	36.4 ± 2.27***	54.4 ± 1.53***	0.7 ± 0.03***
Δ*aat1*	16.7 ± 0.86**	31.7 ± 1.40	0.5 ± 0.05***
Mitochondria			
WT	4.1 ± 0.36	<0.5	>10
Δ*yfh1*	5.0 ± 0.30*	<0.5	>10
Δ*aat1*	5.6 ± 0.49*	<0.5	>10

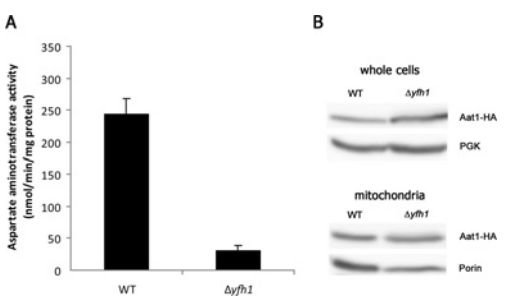

Figure 4 Post-translational inactivation of Aat1 in Δ*yfh1* cells

(**A**) Activity of Aat1–HA in wild-type and mutant mitochondria. (**B**) Proteins from whole cells and mitochondria were analysed by immunoblotting using anti-HA, anti-(phosphoglycerate kinase) (PGK) and anti-porin antibodies.

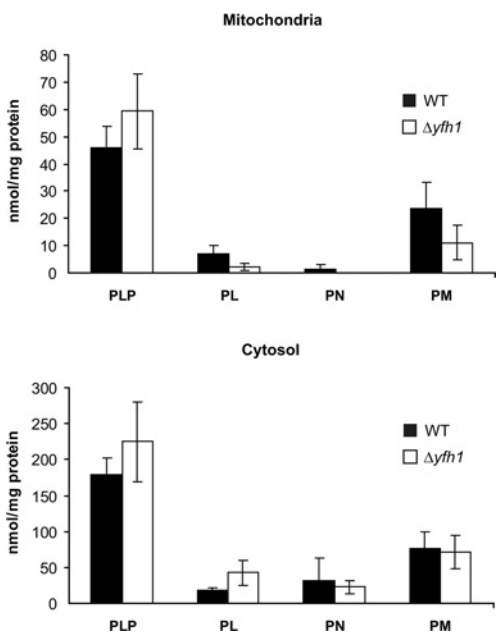

Figure 5 Vitamin B_6 pools in Δ*yfh1* and wild-type cells

PLP, PL, PN and PM levels were determined by HPLC in mitochondrial and cytosolic fractions. Results are means ± S.D. ($n = 3$).

with decreased pI (Figure 6A), which are compatible with protein modification by phosphorylation or acetylation. Treatment of wild-type and Δ*yfh1* mitochondrial samples with alkaline phosphatase did not reveal any Aat1 pattern change in SDS/PAGE or 2D gel electrophoresis (results not shown). We then tested for acetylation/deacetylation modifications. The human mitochondrial aspartate aminotransferase (Got2) has

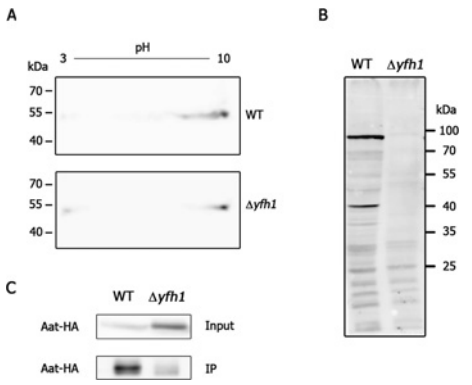

Figure 6 Mitochondrial aspartate aminotransferase is deacetylated in Δ*yfh1* cells

(**A**) Protein separation from mitochondrial fraction by 2D gel electrophoresis and immunodetection using anti-HA antibody. (**B**) Mitochondrial acetyl proteome detected by Western blotting using an anti-(acetylated lysine) antibody. (**C**) Mitochondrial proteins were immunoprecipitated using anti-(acetylated lysine) antibody and Aat1 was immunodetected using anti-HA antibody.

eight putative acetylation sites (Lys^{73}, Lys^{90}, Lys^{150}, Lys^{159}, Lys^{234}, Lys^{296}, Lys^{396} and Lys^{404}; http://www.phosida.com; [34]). Although no acetylation site is predicted for the Aat1 amino acid sequence, Got2 Lys^{73} is conserved in Aat1 (Lys^{60}). Recently, Morselli et al. [35] showed that treatment of human colon carcinoma HCT 116 cells with resveratrol and spermidine elicit deacetylation of Got2 Lys^{73}. In addition, Got2 has also been found to be acetylated in human liver tissue (Lys^{150} and Lys^{309}) [36]. It is thus possible that the acetylation status of Aat1 is modified in Δ*yfh1* cells. The mitochondrial proteome of Δ*yfh1* samples showed a substantial reduction in the amount of acetylated proteins as evidenced by detection in Western blots using anti-(acetylated lysine) antibodies (Figure 6B). Protein acetylation and deacetylation is catalysed by protein lysine acetyltransferases (formerly termed histone acetyltransferases) and protein lysine deacetylases (formerly termed histone deacetylases) respectively [37]. Protein acetyltransferases transfer an acetyl group from acetyl-CoA to form ε-*N*-acetyl-lysine. In agreement with the observation that mitochondrial proteins of Δ*yfh1* cells are less acetylated, the mitochondrial levels of acetyl-CoA and CoA were reduced in this mutant compared with wild-type (CoA, 0.07 ± 0.005 nmol/mg of protein in Δ*yfh1* and 0.11 ± 0.014 nmol/mg of protein in wild-type; acetyl-CoA, 1.54 ± 0.111 pmol/mg of protein in Δ*yfh1* and 2.09 ± 0.293 pmol/mg of protein in wild-type). Immunoprecipitation of mitochondrial acetylated proteins followed by detection of Aat1–HA using an anti-HA antibody revealed that the amount of protein detected in Δ*yfh1* was considerably reduced compared with wild-type (Figure 6C). These results suggest that Aat1 was subjected to post-translational modifications (deacetylation) that may possibly lead to inactivation.

DISCUSSION

The regulation of cellular NAD and NADP pools is essential for energy metabolism, regulation of antioxidant capacity and generation of ROS, which correspond to major functions affected in frataxin-deficient cells. In the present study, we show that, although the NAD^+/NADH ratio is decreased, the total $NAD^+ + NADH$ level is higher in Δ*yfh1* compared with wild-type cells. This could result from oxidative stress state, phosphate deficiency and/or Aat1 inactivation. Increased overall cellular concentration of NAD is in apparent contradiction with the respiratory defect observed in the Δ*yfh1* mutant. However, it was observed that an increase or a decrease in mitochondrial NAD content by modulation of the expression of Ndt1/2 carriers results in reduced cellular ATP content under full respiratory conditions [31]. In the conditions used in the present study of high-glucose media and aerobiosis, the metabolism of Δ*yfh1* cells is shifted to alcohol fermentation. The alcohol dehydrogenase shuttle is activated in Δ*yfh1* possibly to compensate for the blockage of the tricarboxylic acid cycle due to loss of aconitase and succinate dehydrogenase activities, reduced malate dehydrogenase activity and inhibition of the malate–aspartate shuttle.

The *S. cerevisiae* electron transport chain lacks complex I. As an alternative, an inner mitochondrial membrane NADH dehydrogenase, Ndi1, and two external NADH dehydrogenases, Nde1 and Nde2, transfer electrons directly from the matrix and cytosolic NADH to ubiquinone. Under aerobic conditions, external NADH dehydrogenases and the glycerol 3-phosphate shuttle are the most important mechanisms for mitochondrial oxidation of cytosolic NADH [13,14]. For this reason, the physiological significance of the malate–aspartate shuttle in yeast metabolism has long been questioned. The identification of the mitochondrial aspartate/glutamate transporter Agc1 provided strong evidence for the existence of this shuttle [15]. Later, the mitochondrial components of the malate–aspartate shuttle were shown to play a major role in calorie restriction-induced lifespan extension in yeast [16]. Our results showing the reduced respiratory activity of Δ*aat1* mutant further demonstrate the importance of the malate–aspartate shuttle in energy metabolism in yeast.

The finding that the malate–aspartate shuttle is inhibited in Δ*yfh1* cells raises the question of whether its activity is also altered in frataxin-deficient human cells. The malate–aspartate shuttle is quantitatively the most important in the brain, in pancreatic β-cells and in almost all vertebrate tissues [38]. This redox shuttle is composed of cytosolic and mitochondrial aspartate aminotransferases and malate dehydrogenases, the malate 2-oxoglutarate carrier and two calcium-sensitive aspartate/glutamate carriers, Aralar1 (primarily expressed in skeletal muscle, brain and pancreatic β-cells) and citrin (primarily expressed in liver and kidneys). In pancreatic β-cells, coupling of glycolysis to the TCA cycle and electron transport chain is necessary for glucose-induced insulin secretion. It is thus not surprising that the NADH redox shuttles play a significant role in the regulation of insulin secretion [38]. Overexpression of Aralar1 enhances mitochondrial metabolism and insulin secretion [39]. Inversely, disruption of the glycerol 3-phosphate and the malate–aspartate shuttles in mice lead to suppression of glucose-induced increase in NADH and ATP and insulin secretion [40]. A high percentage of FA patients present Type 2 diabetes involving deterioration of the capacity of insulin release and action [1]. This is a late clinical feature, generally diagnosed after onset of neurological disability [41]. It is possible that the malate–aspartate redox shuttle is affected in pancreatic β-cells from patients contributing to the emergence of diabetes.

Reversible lysine acetylation is conserved from prokaryotes to humans [42]. This post-translational modification has been extensively studied for histones, where it plays a key role in the regulation of chromatin dynamics and gene expression. Proteomic analysis using several mammalian cell lines, mouse and human liver and bacteria revealed that not only are nuclear proteins acetylated, but numerous cytosolic and mitochondrial proteins are also acetylated [35,36,42–45]. In particular, metabolic enzymes are extensively acetylated suggesting that this post-translational

modification has a potential regulatory role. Indeed, alterations in the availability of extracellular nutrients induce variations in the degree of enzyme acetylation [36]. Acetylated enzymes belong to different pathways such as glycolysis, gluconeogenesis, the TCA cycle, fatty acid oxidation, glycogen metabolism, the urea cycle, amino acid metabolism and oxidative phosphorylation [37]. In human liver, all enzymes of the TCA cycle and a large proportion of glycolysis enzymes are acetylated [36]. The relationship between acetylation and activity has only been investigated in a small number of enzymes, and it appears that acetylation can affect protein stability and activity, by either increasing or decreasing it [36,44]. Mitochondrial malate dehydrogenase participates in the TCA cycle and the malate–aspartate NADH shuttle. In human liver, this enzyme has four acetylated lysines residues and activity was increased by acetylation [36]. Excluding reports concerning chromatin and gene transcription, nothing is known on the subject of lysine acetylation of yeast proteins. However, since metabolic enzymes of organisms as distant as bacteria and human are acetylated, it is expected that the metabolism of yeast cells is also regulated by acetylation/deacetylation. A general decrease in acetylation was observed for mitochondrial proteins of molecular mass higher than 25 kDa in Δ*yfh1* cells. It is possible that a decrease in acetylation causes a reduction in malate dehydrogenase activity. Aspartate aminotransferase was also found to be active only in wild-type mitochondria where the acetylation level is high. It is tempting to speculate that the mitochondrial components of the malate–aspartate NADH shuttle are regulated by acetylation/deacetylation.

In yeast mitochondria, nothing is known about the enzymes responsible for the lysine-acetyltransferase and lysine-deacetylation activities. In mammalian cells, several members of the SIRT NAD^+-dependent protein deacetylase family are localized in the mitochondria (SIRT3/4/5) [46]. Results obtained from deletion of the *Sirt3* gene in mouse revealed a global alteration of protein acetylation, thus suggesting that SIRT3 is a major deacetylase in the mitochondria [47]. SIRTs and the Sir2 yeast homologue use NAD^+ as an obligatory substrate in the deacetylation reaction. It is proposed that a high ratio of cellular NAD^+/NADH activates Sir2 during calorie restriction as a result of increased respiratory activity [48]. A similar proposition has been made for mammalian SIRTs [37]. In Δ*yfh1* cells, a decrease in the NAD^+/NADH ratio is observed in addition to hypoacetylation of mitochondrial proteins. This is not compatible with what is known about the regulation of deacetylases activity. Another hypothesis is that acetyltransferase activity is reduced in Δ*yfh1*; this would be consistent with the metabolic shift towards alcohol fermentation and reduction of acetyl-CoA levels and the TCA cycle.

Frataxin-deficient cells from all eukaryotic organisms studied have pleiotropic phenotypes [6]. It is recognized that assembly of iron–sulfur clusters is the primary function affected as well as the contribution of oxidative stress hypersensitivity and disruption of iron homoeostasis. Post-translational modifications of proteins allow regulation of important cellular functions that could strengthen or generate new phenotypes in frataxin-deficient cells. In the present study, we found that mitochondrial protein acetylation is modified in the Δ*yfh1* mutant, which could result in deacetylation of Aat1 and its inactivation, exacerbating the respiratory deficiency. Other protein modifications have been observed in frataxin-deficient cells. The glutathionylation of actin alters cytoskeletal dynamics impairing the induction of the Nrf2-dependent Phase II antioxidant pathway in fibroblasts from FA patients [49,50]. These results draw attention to the importance of post-translational protein modifications in frataxin-deficient cells and the need to expand our knowledge in this area to better understand the physiopathology of FA.

AUTHOR CONTRIBUTION

Dominika Sliwa designed the study, performed the experiments, analysed the results and prepared the Figures. Renata Santos designed the study, was involved in all aspects of the experiments, analysed the results and wrote the paper. Julien Dairou was responsible for the HPLC metabolite analysis and commented on the paper. Jean-Michel Camadro started the project, discussed the results and commented on the paper.

ACKNOWLEDGEMENT

We acknowledge the help of the technical platform 'BioProfiler-UFLC'.

FUNDING

This work was supported by Association Française Ataxie de Friedreich (AFAF), France and by the 'Agence Nationale de la Recherche' ('ANR Maladies Rares'), France [grant number ANR-06-MRAR-025-01]. D.S. received a Ph.D. fellowship from AFAF.

REFERENCES

1 Koeppen, A. H. (2011) Friedreich's ataxia: pathology, pathogenesis, and molecular genetics. J. Neurol. Sci. **303**, 1–12
2 Wells, R. D. (2008) DNA triplexes and Friedreich ataxia. FASEB J. **22**, 1625–1634
3 Hebert, M. D. (2008) Targeting the gene in Friedreich ataxia. Biochimie **90**, 1131–1139
4 Campuzano, V., Montermini, L., Molto, M. D., Pianese, L., Cossée, M., Cavalcanti, F., Monros, E., Rodius, F., Duclos, F., Monticelli, A. et al. (1996) Friedreich's ataxia: autosomal recessive disease caused by an intronic GAA triplet repeat expansion. Science **271**, 1423–1427
5 Stemmler, T. L., Lesuisse, E., Pain, D. and Dancis, A. (2010) Frataxin and mitochondrial FeS cluster biogenesis. J. Biol. Chem. **285**, 26737–26743
6 Santos, R., Lefevre, S., Sliwa, D., Seguin, A., Camadro, J. M. and Lesuisse, E. (2010) Friedreich ataxia: molecular mechanisms, redox considerations and therapeutic opportunities. Antioxid. Redox Signaling **13**, 651–690
7 Auchère, F., Santos, R., Planamente, S., Lesuisse, E. and Camadro, J. M. (2008) Glutathione-dependent redox status of frataxin-deficient cells in a yeast model of Friedreich's ataxia. Hum. Mol. Genet. **17**, 2790–2802
8 Schulz, T. J., Westermann, D., Isken, F., Voigt, A., Laube, B., Thierbach, R., Kuhlow, D., Zarse, K., Schomburg, L., Pfeiffer, A. F. et al. (2010) Activation of mitochondrial energy metabolism protects against cardiac failure. Aging **2**, 843–853
9 Houtkooper, R. H., Cantó, C., Wanders, R. J. and Auwerx, J. (2010) The secret life of NAD^+: an old metabolite controlling new metabolic signaling pathways. Endocr. Rev. **31**, 194–223
10 Ying, W. (2008) NAD^+/NADH and $NADP^+$/NADPH in cellular functions and cell death: regulation and biological consequences. Antioxid. Redox Signaling **10**, 179–206
11 Szappanos, B., Kovács, K., Szamecz, B., Honti, F., Costanzo, M., Baryshnikova, A., Gelius-Dietrich, G., Lercher, M. J., Jelasity, M., Myers, C. L. et al. (2011) An integrated approach to characterize genetic interaction networks in yeast metabolism. Nat. Genet. **43**, 656–662
12 Todisco, S., Agrimi, G., Castegna, A. and Palmieri, F. (2006) Identification of the mitochondrial NAD^+ transporter in *Saccharomyces cerevisiae*. J. Biol. Chem. **281**, 1524–1531
13 Bakker, B. M., Overkamp, K. M., van Maris, A., Kötter, P., Luttik, M. A., van Dijken, J. P. and Pronk, J. T. (2001) Stoichiometry and compartmentation of NADH metabolism in *Saccharomyces cerevisiae*. FEMS Microbiol. Rev. **25**, 15–37
14 Rigoulet, M., Aguilaniu, H., Avéret, N., Bunoust, O., Camougrand, N., Grandier-Vazeille, X., Larsson, C., Pahlman, I. L., Manon, S. and Gustafsson, L. (2004) Organization and regulation of the cytosolic NADH metabolism in the yeast *Saccharomyces cerevisiae*. Mol. Cell. Biochem. **256/257**, 73–81
15 Cavero, S., Vozza, A., del Arco, A., Palmieri, L., Villa, A., Blanco, E., Runswick, M. J., Walker, J. E., Cerdán, S., Palmieri, F. and Satrústegui, J. (2003) Identification and metabolic role of the mitochondrial aspartate-glutamate transporter in *Saccharomyces cerevisiae*. Mol. Microbiol. **50**, 1257–1269
16 Easlon, E., Tsang, F., Skinner, C., Wang, C. and Lin, S. J. (2008) The malate–aspartate NADH shuttle components are novel metabolic longevity regulators required for calorie restriction-mediated life span extension in yeast. Genes Dev. **22**, 931–944

17 Ramos, M., Pardo, B., Llorente-Folch, I., Saheki, T., Del Arco, A. and Satrústegui, J. (2011) Deficiency of the mitochondrial transporter of aspartate/glutamate aralar/AGC1 causes hypomyelination and neuronal defects unrelated to myelin deficits in mouse brain. J. Neurosci. Res. **89**, 2008–2017

18 Li, J., Kogan, M., Knight, S. A., Pain, D. and Dancis, A. (1999) Yeast mitochondrial protein, Nfs1p, coordinately regulates iron-sulfur cluster proteins, cellular iron uptake, and iron distribution. J. Biol. Chem. **274**, 33025–33034

19 Zhang, Y., Lyver, E. R., Knight, S. A., Lesuisse, E. and Dancis, A. (2005) Frataxin and mitochondrial carrier proteins, Mrs3p and Mrs4p, cooperate in providing iron for heme synthesis. J. Biol. Chem. **280**, 19794–19807

20 Gale, C., Gerami-Nejad, M., McClellan, M., Vandoninck, S., Longtine, M. S. and Berman, J. (2001) *Candida albicans* Int1p interacts with the septin ring in yeast and hyphal cells. Mol. Biol. Cell **12**, 3538–3549.

21 Bulteau, A. L., Ikeda-Saito, M. and Szweda, L. I. (2003) Redox-dependent modulation of aconitase activity in intact mitochondria. Biochemistry **42**, 14846–14855

22 Munujos, P., Coll-Cantí, J., González-Sastre, F. and Gella, F. J. (1993) Assay of succinate dehydrogenase activity by a colorimetric-continuous method using iodonitrotetrazolium chloride as electron acceptor. Anal. Biochem. **212**, 506–509

23 Bisp, M. R., Bor, M. V., Heinsvig, E. M., Kall, M. A. and Nexø, E. (2002) Determination of vitamin B6 vitamers and pyridoxic acid in plasma: development and evaluation of a high-performance liquid chromatographic assay. Anal. Biochem. **305**, 82–89

24 Seguin, A., Santos, R., Pain, D., Dancis, A., Camadro, J. M. and Lesuisse, E. (2011) Co-precipitation of phosphate and iron limits mitochondrial phosphate availability in *Saccharomyces cerevisiae* lacking the yeast frataxin homologue (*YFH1*). J. Biol. Chem. **286**, 6071–6079

25 Pfaffl, M. W. (2001) A new mathematical model for relative quantification in real-time RT-PCR. Nucleic Acids Res. **29**, e45–e50

26 Chen, O. S., Hemenway, S. and Kaplan, J. (2002) Inhibition of Fe-S cluster biosynthesis decreases mitochondrial iron export: evidence that Yfh1p affects Fe-S cluster synthesis. Proc. Natl. Acad. Sci. U.S.A. **99**, 12321–12326

27 Philpott, C. C. and Protchenko, O. (2008) Response to iron deprivation in *Saccharomyces cerevisiae*. Eukaryotic Cell **7**, 20–27

28 Castegna, A., Scarcia, P., Agrimi, G., Palmieri, L., Rottensteiner, H., Spera, I., Germinario, L. and Palmieri, F. (2010) Identification and functional characterization of a novel mitochondrial carrier for citrate and oxoglutarate in *Saccharomyces cerevisiae*. J. Biol. Chem. **285**, 17359–17370

29 Minard, K. I. and McAlister-Henn, L. (2010) Pnc1p supports increases in cellular NAD(H) levels in response to internal or external oxidative stress. Biochemistry **49**, 6299–6301

30 Lu, S. P. and Lin, S. J. (2011) Phosphate-responsive signaling pathway is a novel component of NAD^+ metabolism in *Saccharomyces cerevisiae*. J. Biol. Chem. **286**, 14271–14281

31 Agrimi, G., Brambilla, L., Frascotti, G., Pisano, I., Porro, D., Vai, M. and Palmieri, L. (2011) Deletion or overexpression of mitochondrial NAD^+ carriers in *Saccharomyces cerevisiae* alters cellular NAD and ATP contents and affects mitochondrial metabolism and the rate of glycolysis. Appl. Environ. Microbiol. **77**, 2239–2246

32 Mooney, S. and Hellmann, H. (2010) Vitamin B6: killing two birds with one stone? Phytochemistry **71**, 495–501

33 Voziyan, P. A. and Hudson, B. G. (2005) Pyridoxamine as a multifunctional pharmaceutical: targeting pathogenic glycation and oxidative damage. Cell. Mol. Life Sci. **62**, 1671–1681

34 Gnad, F., Gunawardena, J. and Mann, M. (2011) PHOSIDA 2011: the posttranslational modification database. Nucleic Acids Res. **39**, D253–D260

35 Morselli, E., Mariño, G., Bennetzen, M. V., Eisenberg, T., Megalou, E., Schroeder, S., Cabrera, S., Bénit, P., Rustin, P., Criollo, A. et al. (2011) Spermidine and resveratrol induce autophagy by distinct pathways converging on the acetylproteome. J. Cell Biol. **192**, 615–629

36 Zhao, S., Xu, W., Jiang, W., Yu, W., Lin, Y., Zhang, T., Yao, J., Zhou, L., Zeng, Y., Li, H. et al. (2010) Regulation of cellular metabolism by protein lysine acetylation. Science **327**, 1000–1004

37 Guan, K. L. and Xiong, Y. (2011) Regulation of intermediary metabolism by protein acetylation. Trends Biochem. Sci. **36**, 108–116

38 Bender, K., Newsholme, P., Brennan, L. and Maechler, P. (2006) The importance of redox shuttles to pancreatic β-cell energy metabolism and function. Biochem. Soc. Trans. **34**, 811–814

39 Rubi, B., del Arco, A., Bartley, C., Satrustegui, J. and Maechler, P. (2004) The malate–aspartate NADH shuttle member Aralar1 determines glucose metabolic fate, mitochondrial activity, and insulin secretion in beta cells. J. Biol. Chem. **279**, 55659–55666

40 Eto, K., Tsubamoto, Y., Terauchi, Y., Sugiyama, T., Kishimoto, T., Takahashi, N., Yamauchi, N., Kubota, N., Murayama, S., Aizawa, T. et al. (1999) Role of NADH shuttle system in glucose-induced activation of mitochondrial metabolism and insulin secretion. Science **283**, 981–985

41 Podolsky, S. and Sheremata, W. A. (1970) Insulin-dependent diabetes mellitus and Friedreich's ataxia in siblings. Metab., Clin. Exp. **19**, 555–561

42 Choudhary, C., Kumar, C., Gnad, F., Nielsen, M. L., Rehman, M., Walther, T. C., Olsen, J. V. and Mann, M. (2009) Lysine acetylation targets protein complexes and co-regulates major cellular functions. Science **325**, 834–840

43 Kim, S. C., Sprung, R., Chen, Y., Xu, Y., Ball, H., Pei, J., Cheng, T., Kho, Y., Xiao, H., Xiao, L. et al. (2006) Substrate and functional diversity of lysine acetylation revealed by a proteomics survey. Mol. Cell **23**, 607–618

44 Wang, Q., Zhang, Y., Yang, C., Xiong, H., Lin, Y., Yao, J., Li, H., Xie, L., Zhao, W., Yao, Y. et al. (2010) Acetylation of metabolic enzymes coordinates carbon source utilization and metabolic flux. Science **327**, 1004–1007

45 Zhang, J., Sprung, R., Pei, J., Tan, X., Kim, S., Zhu, H., Liu, C. F., Grishin, N. V. and Zhao, Y. (2009) Lysine acetylation is a higly abundant and evolutionary conserved modification in *Escherichia coli*. Mol. Cell. Proteomics **8**, 215–225

46 Michishita, E., Park, J. Y., Burneskis, J. M., Barrett, J. C. and Horikawa, I. (2005) Evolutionarily conserved and nonconserved cellular localizations and functions of human SIRT proteins. Mol. Biol. Cell **16**, 4623–4635

47 Lombard, D. B., Alt, F. W., Cheng, H., Bunkenborg, J., Streeper, R. S., Mostoslavsky, R., Kim, J., Yancopoulos, G., Valenzuela, D., Murphy, A. et al. (2007) Mammalian Sir2 homolog SIRT3 regulates global mitochondrial lysine acetylation. Mol. Cell. Biol. **27**, 8807–8814

48 Lin, S. J., Ford, E., Haigis, M., Liszt, G. and Guarente, L. (2004) Calorie restriction extends yeast life span by lowering the level of NADH. Genes Dev. **18**, 12–16

49 Paupe, V., Dassa, E., Goncalves, S., Auchère, F., Lönn, M., Holmgren, A. and Rustin, P. (2009) Impaired nuclear Nrf2 translocation undermines the oxidative stress response in Friedreich ataxia. PLoS ONE **4**, e4253

50 Pastore, A., Tozzi, G., Gaeta, L. M., Bertini, E., Serafini, V., Di Cesare, S., Bonetto, V., Casoni, F., Carrozzo, R., Federici, G. and Piemonte, F. (2003) Actin glutathionylation increases in fibroblasts of patients with Friedreich's ataxia: a potential role in the pathogenesis of the disease. J. Biol. Chem. **278**, 42588–42595

Received 30 August 2011/20 October 2011; accepted 20 October 2011
Published as BJ Immediate Publication 20 October 2011, doi:10.1042/BJ20111574